

Effect of pressure on the spin-polarized intergrain tunneling in single and polycrystalline $\text{Sr}_2\text{FeMoO}_6$

S. Kaji and G. Oomi

Department of Physics, Kyushu University, Ropponmatsu, Chuo-ku, Fukuoka 810-8560, Japan

Y. Tomioka

Correlated Electron Research Center (CERC), National Institute of Advanced Industrial Science and Technology (AIST), Tsukuba 305-0046, Japan

Y. Tokura

Department of Applied Physics, University of Tokyo, Tokyo 113-8656, Japan

(Received 16 November 2005; revised manuscript received 20 August 2006; published 25 January 2007)

The electrical resistivity and magnetoresistance (MR) have been measured under high pressure using single and polycrystalline samples of $\text{Sr}_2\text{FeMoO}_6$. It is found that the intrinsic negative MR in the single crystal is not affected by applying pressure. However, the MR in polycrystalline samples exhibits two distinct pressure dependences, a strong pressure dependence at low field below 2 T and small changes at high field above 2 T. These findings indicate that, in this material, the large MR at low field is dominated by spin-polarized tunneling between grains and is strongly suppressed by applying pressure.

DOI: [10.1103/PhysRevB.75.024430](https://doi.org/10.1103/PhysRevB.75.024430)

PACS number(s): 74.62.Fj, 75.47.De, 73.40.-c

I. INTRODUCTION

The intergranular magnetoresistance in half-metallic granular systems has attracted great interest since the discovery of low-field magnetoresistance in polycrystalline samples of the perovskite manganite. In the ferromagnetic ground state of manganites (e.g., $\text{La}_{1/2}\text{Sr}_{1/3}\text{MnO}_3$), the density of states near the Fermi level is composed only of up-spin e_g electrons. That is, a half-metallic nature is realized, which allows spin-dependent carrier scattering processes at the tunnel junctions, twin boundaries in the crystal, and grain boundaries in polycrystalline ceramics.¹⁻³

As it has been indicated in Ref. 4, such a half-metallic state is also realized in complex oxides with the ordered perovskite structure, A_2FeMoO_6 ($\text{A}=\text{Ca}$, Sr , and Ba). $\text{Sr}_2\text{FeMoO}_6$ has long been known as a conducting ferromagnet (or ferrimagnet) with fairly high magnetic transition temperature around 410–460 K. The occupied up-spin band mainly comes from the Fe 3d electrons, and the Fermi level exists within the down-spin band composed of Fe t_{2g} and Mo t_{2g} electrons. As an intuitive picture for the electronic state, the electrons of Fe and Mo cations may be considered as localized and itinerant, respectively, with the valence states of Fe^{3+} ($3d^5; t_{2g}^3 e_g^2, S=5/2$) and Mo^{5+} ($4d^1; t_{2g}^1, S=1/2$). In a polycrystal of $\text{Sr}_2\text{FeMoO}_6$,⁴ as a result, a fairly large magnetoresistance (MR) due to the intergrain tunneling of spin-polarized electrons has been reported. In Ref. 5, it has been shown that a different thermal treatment of annealing modifies the transport phenomena including the intergrain tunneling MR. These results as indicated in Refs. 4 and 5 suggest that the intergrain tunneling MR is strongly dependent on the properties of the grain boundaries, which can be changed by the preparation conditions.

Application of hydrostatic pressure on polycrystalline samples can change the coupling between grains, which also affects the intergrain tunneling MR. In this paper, we report

the pressure effects on the magnetotransport properties of both a polycrystalline sample and a single crystal of $\text{Sr}_2\text{FeMoO}_6$. We quantitatively analyze the pressure-dependent MR of the polycrystalline sample in comparison with that of the single crystal. It is found that for the single crystal no significant pressure effect is seen on the MR while for the polycrystalline sample the magnitude of MR is suppressed significantly by pressure. These facts further make clear the role of grain boundaries in intergrain tunneling MR in the polycrystalline sample of $\text{Sr}_2\text{FeMoO}_6$. The format of this paper is as follows. The experimental procedure is described in Sec. II and then the pressure effects on the MR and temperature profiles of resistivity are shown for both the single crystal and the polycrystalline sample in Sec. III. Subsequently, a quantitative analysis of the pressure-dependent MR is shown for the polycrystalline sample in Sec. IV. The summary is given in Sec. V.

II. EXPERIMENTAL PROCEDURE

The polycrystalline sample of $\text{Sr}_2\text{FeMoO}_6$ was prepared by the solid-state reaction process described in Ref. 6, and the single crystal was prepared by the floating zone method.⁷ In this paper, an annealed single crystal was used in which the Fe and Mo ordering was about 92%.⁷ The temperature dependence of electrical resistivity was measured using a dc four-terminal method. The magnetic field at 4.2 K was generated by using a superconducting magnet and the maximum applied field was 7 T. We used a cryogen-free magnet to generate the magnetic field above 77 K. Hydrostatic pressure was generated up to 3 GPa by a piston-cylinder device utilizing the conventional Teflon-cell technique. The pressure inside the cell was always kept constant by controlling the load of the hydraulic press within $\pm 5\%$ throughout the measurement. The details of the present pressure apparatus were reported previously.⁸

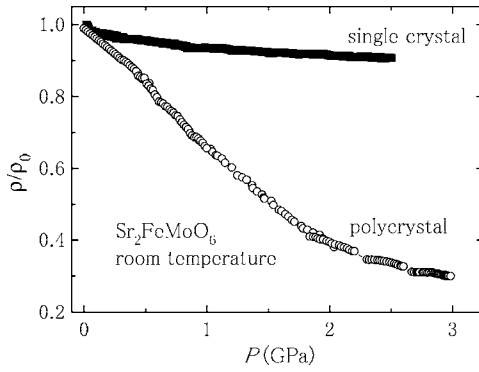


FIG. 1. Pressure dependence of the normalized resistivity (ρ/ρ_0) at room temperature for both the single crystal and the polycrystalline sample. ρ_0 is the resistivity at ambient pressure.

III. RESULTS

Figure 1 shows the electrical resistivities of the single and polycrystalline samples as a function of pressure, normalized to the resistivity at 0 GPa. It is found that the resistivity of polycrystalline sample is decreased by applying pressure at the rate $1/\rho(\partial\rho/\partial P) = -0.33 \text{ GPa}^{-1}$, which is larger than that of the single crystal [$1/\rho(\partial\rho/\partial P) = -0.042 \text{ GPa}^{-1}$]. The resistivity of the polycrystalline sample ($\sim 7 \times 10^{-3} \Omega \text{ cm}$) is an order of magnitude larger than that of the single crystal ($\sim 6 \times 10^{-4} \Omega \text{ cm}$), which seems to be too high for a metallic state. This indicates that the resistance of the polycrystalline sample is dominated by the scattering of carriers at grain boundaries, as widely seen for polycrystalline ceramic samples.^{1,9,10} These facts imply that pressure affects mainly not the bulk properties but the grain boundary. After releasing pressure, the resistivity is the same as that before pressurizing within the experimental error. This fact indicates that the pressure effect on the grain boundaries is reversible below 3 GPa.

Figure 2 shows the temperature profiles of resistivity [$\rho(T)$] under several applied pressures for a single crystal (a) and polycrystalline sample (b), respectively. In Fig. 2(a), the resistivity shows metallic behavior down to 4.2 K at 0.1 GPa (nearly ambient pressure), and no significant pressure effect is observed except for a small decrease of resistivity around room temperature. In Fig. 2(a), we could not see anisotropy in the temperature profiles of resistivity. In Fig. 2(b), on the other hand, the resistivity at 0.1 GPa shows a gradual increase as temperature decreases, although the resistivity at the lowest temperature is not as high as that for a semiconductor. As the pressure increases, a distinct decrease in resistivity is seen for the whole temperature range, and the increase in the magnitude of $\rho(T)$ between room temperature and 4.2 K is also suppressed. As a result, the value of the resistivity at 4.2 K under 3 GPa is decreased to be nearly a quarter of that under 0.1 GPa. There are small kinks in the $\rho(T)$ curves above 1.7 GPa in this figure around 250 K. They might be due to the effect of melting of the pressure medium although the details are not known at present. But the results and discussion are not affected by the existence of these small kinks.

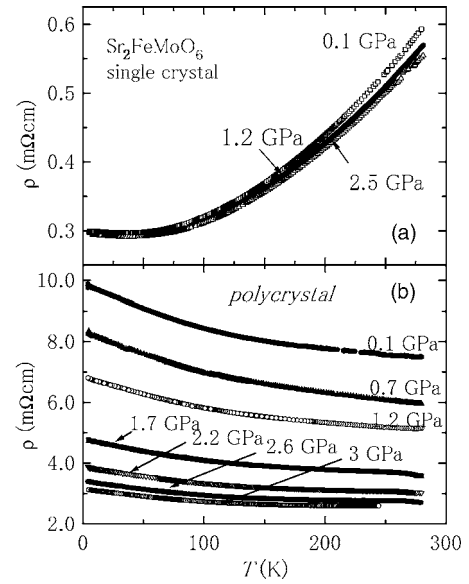


FIG. 2. Temperature profiles of resistivity under several applied pressures for both (a) the single crystal and (b) the polycrystalline sample.

In Fig. 2(b), the $\rho(T)$ curve does not show metallic behavior even at 3 GPa but seems to be semiconducting, where the magnitude of ρ increases with decreasing temperature. In order to examine the temperature dependence in detail, we attempted to fit the $\rho(T)$ curve to the well-known activated type or variable-range-hopping type. It is found that the $\rho(T)$ curve at ambient pressure obeys neither the T^{-1} nor $T^{-1/4}$ law. This fact implies that the semiconductinglike behavior in the polycrystalline sample originates from another mechanism. García-Hernández *et al.*⁹ have explained the difference between single and polycrystalline $\text{La}_{2/3}\text{Ca}_{1/3}\text{MnO}_3$ by comparing with granular metals embedded within an insulating matrix. They suggested a two-channel model: there are poor and good contacts between grains and thus the variation of conductance is dominated by the poorest ones.^{2,9} The connectivity should be understood in a broad sense: it refers not only to the quality of the physical contacts between grains, but also to any alteration of the effective conductance by impurities or defects. Since pressure is considered to make the materials homogeneous, the connection between grains is expected to be enhanced, the resistivity decreases, and the temperature dependence tends to show metallic behavior like that of a single crystal by further pressurizing more than 3 GPa.

Figure 3(a) shows MR $\{=100[\rho(H) - \rho(0)]/\rho(0)\}$ vs H curves of the single crystal with varying pressure from 0.1 to 2.5 GPa, where $\rho(0)$ is the resistivity at zero field. In Fig. 3(a), the MR decreases smoothly with increasing H , and the higher the field the smaller the rate of decrease. It should be noted that the MR vs H curves are almost independent of pressure at least up to 2.5 GPa. In the case of the single crystal, as indicated in Ref. 7, negative MR originating from the antisite defects at the Fe and Mo sites is seen below about 150 K. The result in Fig. 3(a) indicates that application of pressure does not have an effect on the MR relevant to the single crystal.

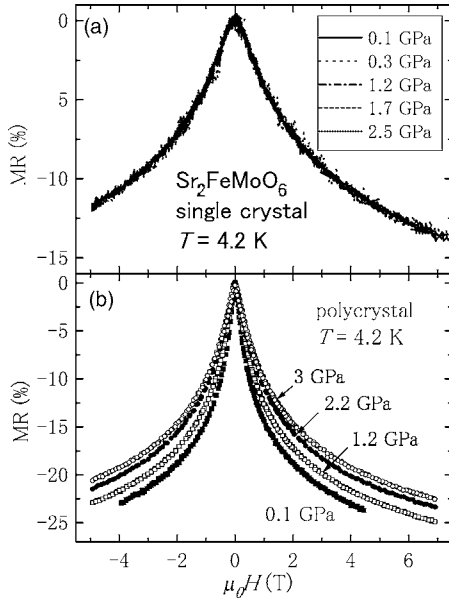


FIG. 3. Magnetoresistance (MR) vs H curves under several applied pressures for (a) a single crystal and (b) a polycrystalline sample, respectively, taken at 4.2 K. The MR is defined as $100[\rho(H) - \rho(0)]/\rho(0)$, where $\rho(0)$ is the resistivity at zero field.

Figure 3(b) shows the MR vs H curves taken at several applied pressures for the polycrystalline sample. In contrast to the case of the single crystal, the MR vs H curves for the polycrystalline sample show significant pressure dependence. The magnitude of the MR decreases with increasing pressure. In Fig. 3(b), the MR near zero field shows a rather rapid decrease, which may be explained by the conduction being dominated by the spin-polarized tunneling between grains associated with the magnetic domain rotation at grain boundaries.¹⁰ At higher fields, however, the rate of decrease of MR becomes smaller, comparable with the case of the single crystal.

Figure 4 shows the MR for a single crystal and a polycrystalline sample at 7 T as a function of pressure. In the

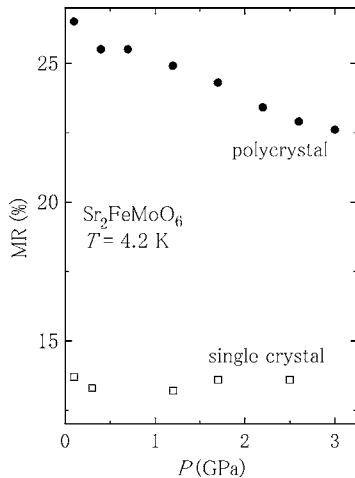


FIG. 4. MR $\{=100[\rho(H) - \rho(0)]/\rho(0)\}$ values at 7 T as a function of pressure for both the single crystal (open squares) and polycrystalline sample (closed circles).

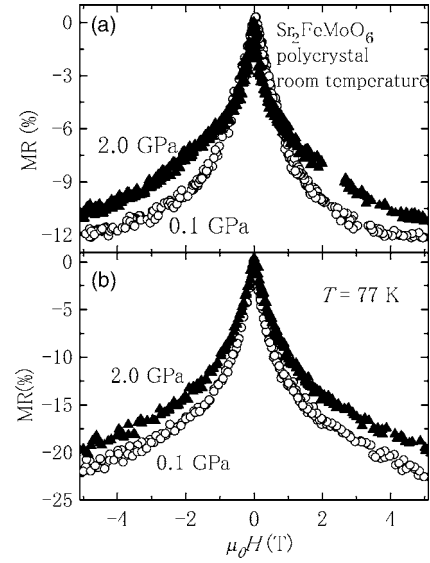


FIG. 5. MR $\{=100[\rho(H) - \rho(0)]/\rho(0)\}$ vs H curves at 0.1 and 2.0 GPa for the polycrystalline sample, taken at (a) room temperature and (b) 77 K.

case of the single crystal, the MR is almost unchanged up to 2.5 GPa, which may be related to the fact that the origin of the small negative MR at low temperature for the single crystal is the antisite defects at the Fe and Mo sites. In the case of the polycrystalline sample, on the other hand, the MR shows a distinct decrease, e.g., from 25.5% at 0.4 GPa to 22.6% at 3 GPa. Since the MR at low field is known to be due to the spin-polarized intergrain tunneling, the decrease of MR originates from a decrease of electron scattering at grain boundaries^{1,4,11} caused by applying pressure.

Figure 5 shows the MR vs H curves at 0.1 and 2.0 GPa for the polycrystalline sample, which are taken at (a) room temperature and (b) 77 K, respectively. The overall features of the MR vs H curves shown in Fig. 5 are similar to those at 4.2 K as shown in Fig. 3(b). The MR values decrease with increasing pressure at both room temperature and 77 K.

IV. DISCUSSION

As indicated in Fig. 3, the MR vs H curves for the single crystal are almost independent of pressure while those for the polycrystalline sample are changed significantly by pressure. In order to study the difference in detail, we show in Fig. 6 the normalized resistivity $[\rho(H)/\rho(0)]$ vs H curves with varying applied pressure for the single crystal (a) and the polycrystalline sample (b). The derivatives of $\rho/\rho(0)$ $d[\rho/\rho(0)]/dH$ are also shown in the insets. In Fig. 6(a), $\rho/\rho(0)$ at 2.5 GPa is quite similar to that at 0.1 GPa, and as shown in the inset, the magnitude of $d[\rho/\rho(0)]/dH$ remains less than 0.05 even at $\mu_0 H \sim 0$. Figure 6(a) again confirms that in the case of the single crystal the magnetotransport is not affected by pressure. In Fig. 6(b), on the other hand, the $\rho/\rho(0)$ vs H curves are strongly dependent on pressure. Furthermore, as shown in the inset of Fig. 6(b), the magnitude of $d[\rho/\rho(0)]/dH$ distinctly increases as the magnetic field ap-

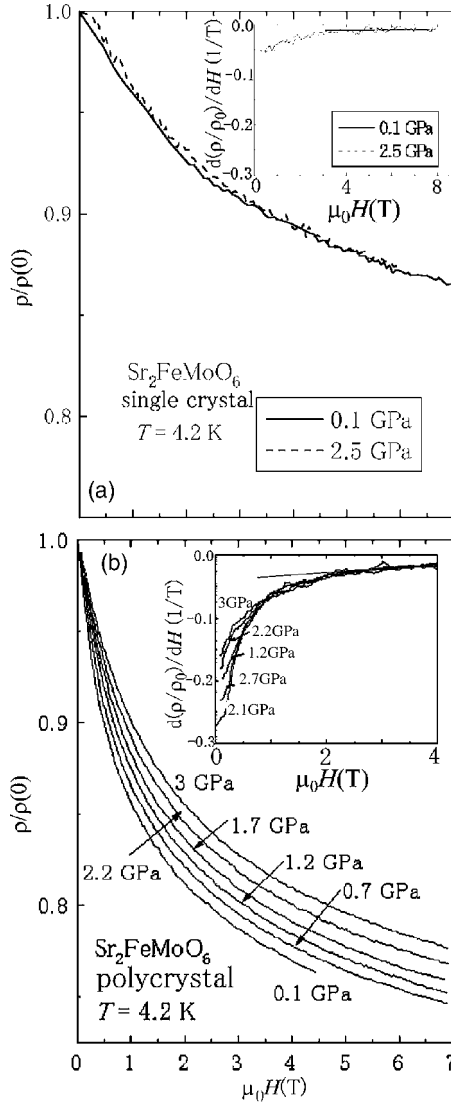


FIG. 6. (a) The normalized resistivity $\rho/\rho(0)$ vs H curves at 0.1 and 2.5 GPa for the single crystal, taken at 4.2 K. (b) The $\rho/\rho(0)$ vs H curves at various pressure (0.1–3 GPa) for the polycrystalline sample, also taken at 4.2 K. The insets show the magnetic field dependence of $d[\rho(H)/\rho(0)]/dH$ for (a) the single crystal and (b) the polycrystalline sample. The lines in the insets are guides to the eyes indicating that $d[\rho(H)/\rho(0)]/dH$ at high fields ($\mu_0 H \gtrsim 2$ T) is linearly dependent on H .

proaches zero, irrespective of the applied pressure. The observed difference in Fig. 6 seems to be attributable to the existence of the grain boundaries in the polycrystalline sample, which gives rise to a large MR effect.

In the insets, the $d[\rho(H)/\rho(0)]/dH$ vs H curves for both the single crystal and the polycrystalline sample become independent of the applied pressure as the magnetic field increases. At high fields ($\mu_0 H \gtrsim 2$ T), the decrease in the magnitude of $d[\rho(H)/\rho(0)]/dH$ may be approximated as linear against H , which indicates that $\rho/\rho(0)$ at high fields should be expressed as $aH + bH^2 + c$. In this paper, however, for simplicity, we roughly approximate $\rho/\rho(0)$ by assuming the following equation:³

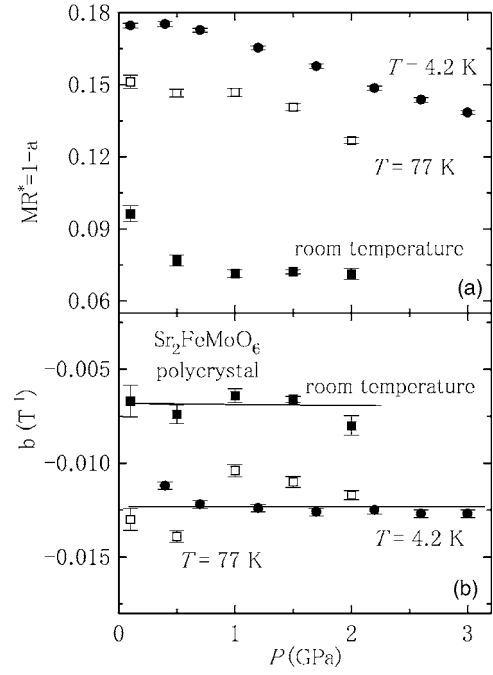


FIG. 7. (a) MR^* (see text) and (b) the high-field MR slope for the polycrystalline sample, plotted against the applied pressure. The values at 4.2 K, 77 K, and room temperature are denoted as closed circles, open squares, and closed squares, respectively.

$$\rho/\rho(0) = a + bH, \quad (1)$$

where a and b are constants depending on temperature and pressure. In this equation, we may estimate the contribution to the MR from the spin-polarized tunneling effect and that from the bulk properties at high fields as $1 - a (=MR^*)$ and b , respectively.

The $\rho/\rho(0)$ vs H curves at the same applied pressure as shown in Fig. 6 are analyzed with use of Eq. (1), and we plot in Figs. 7(a) and 7(b), MR^* and b against the applied pressure, respectively. The same analysis is also applied to the $\rho/\rho(0)$ vs H curves at 77 K and room temperature, the results of which are also plotted in Figs. 7(a) and 7(b). In Fig. 7(a), MR^* at 4.2 K decreases with increasing pressure, and the decreasing rate $(1/MR^*) [d(MR^*)/dP]$ is roughly estimated to be about $-7.6 \times 10^{-2} \text{ GPa}^{-1}$. Similar pressure dependence is also found at 77 K: the pressure coefficient of MR^* is almost the same as that at 4.2 K. At room temperature, the values of MR^* decrease also with increasing pressure. In Fig. 7(a), the MR^* at 4.2 K is about 18% at ambient pressure. In Fig. 4, which is the result at 4.2 K, the MR at 7 T is about 27% at ambient pressure. For the present polycrystalline sample, therefore, the MR from spin-polarized tunneling between grains and that from the bulk properties become about 18% and about 9%, respectively.

In Fig. 7(b), on the other hand, b at the corresponding temperature seems to be almost independent of applied pressure. The value at 4.2 K (about -0.012 T^{-1}) is almost the same as that at 77 K, and it is about -0.006 T^{-1} at room temperature. In the cases of 4.2 and 77 K, since the temperature is well below $T_C (=420 \text{ K})$ and the bulk properties (e.g.,

the saturation magnetization M_s) are almost independent of the temperature, b should also be independent of temperature. The same analysis is also done on the $\rho/\rho(0)$ vs H curves for the single crystal [Fig. 6(a)] and b at 4.2 K is estimated to be about -0.011 , which is nearly the same as that shown in Fig. 7(b). That is, the MR from the bulk properties for the polycrystalline sample is comparable to that for the single crystal. It should also be noticed that for the $\text{Sr}_2\text{FeMoO}_6$ single crystal, T_C and M_s are increased by application of pressure.¹² The coefficient dT_C/dP is about 3–5 K/GPa, and the change in M_s is not more than 1% up to 0.8 GPa. Figure 7(b) indicates that such changes in T_C and M_s due to the application of pressure seem to be too small to noticeably change the value of b .

Figure 8 shows the temperature variation of $MR^*(T)/MR^*(4.2\text{ K})$ at 0.1 and 2 GPa, plotted against the reduced temperature (T/T_C) with $T_C=420$ K. For comparison, the normalized magnetization $M(T)/M(5\text{ K})$ and its square $[M(T)/M(5\text{ K})]^2$ taken at 1 T for the polycrystalline sample are also plotted in the figure. For the present polycrystalline sample, the value of $M(5\text{ K})$ is about $2.9\mu_B/\text{f.u.}$ at 1 T. In the perovskite manganites, as reported in Ref. 3, the temperature variation of MR^* decays much faster than that of the square of magnetization (M^2) and approximately shows linear dependence against T/T_C . In Fig. 8, the $MR^*(T)/MR^*(4.2\text{ K})$ for $\text{La}_{0.35}\text{Pr}_{0.35}\text{Sr}_{0.3}\text{MnO}_3$ and $\text{La}_{0.67}\text{Sr}_{0.33}\text{MnO}_3$ (Ref. 3) are shown for comparison. $MR^*(T)$ of $\text{Sr}_2\text{FeMoO}_6$ seems to decrease as M/M_s rather than $(M/M_s)^2$. Although further study is needed to discuss the temperature variation of MR^* in more detail, the present result as shown in Fig. 8 implies that as temperature increases, the MR^* of the polycrystalline $\text{Sr}_2\text{FeMoO}_6$ might decay more slowly than that of the manganites.

V. CONCLUSION

In summary, we have examined the MRs of single and polycrystalline samples of $\text{Sr}_2\text{FeMoO}_6$ at high pressure. The

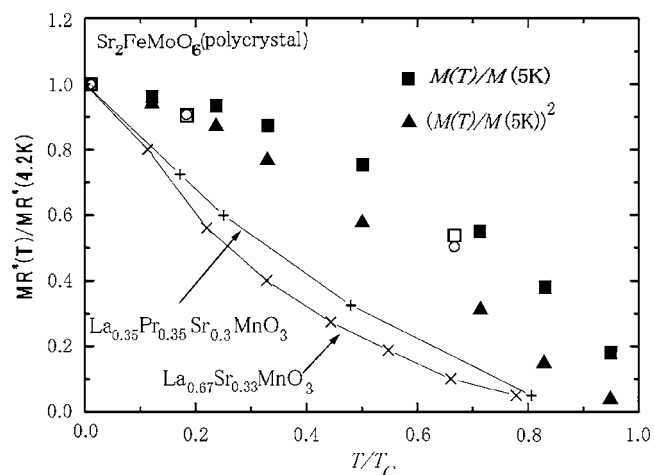


FIG. 8. Temperature variation of $MR^*(T)/MR^*(4.2\text{ K})$ at 0.1 GPa (open squares) and that at 2 GPa (open circles) for the polycrystalline sample, plotted against the reduced temperature (T/T_C) with $T_C=420$ K. The closed squares and triangles denote $M(T)/M(5\text{ K})$ and $[M(T)/M(5\text{ K})]^2$, respectively. The normalized magnetization $M(T)/M(5\text{ K})$ and its square $[M(T)/M(5\text{ K})]^2$ are obtained by the temperature profiles of magnetization at 1 T. The value of $M(5\text{ K})$ is about $2.9\mu_B/\text{f.u.}$ Solid lines are the $MR^*(T)/MR^*(4.2\text{ K})$ of $\text{La}_{0.35}\text{Pr}_{0.35}\text{Sr}_{0.3}\text{MnO}_3$ and $\text{La}_{0.67}\text{Sr}_{0.33}\text{MnO}_3$ for comparison (Ref. 3).

resistivity for the polycrystalline sample decreases rapidly with increasing pressure, which is in contrast to that for the single crystal. The negative MR of the single crystal does not change under high pressure. The MR in the polycrystalline sample is suppressed by pressure, in particular at low field. In this study, the transport properties of the bulk and grain boundaries are examined by application of pressure. The large pressure effects on the tunneling magnetoresistance (TMR) in the polycrystalline sample originate from spin-polarized tunneling at grain boundaries, in sharp contrast to the behavior for a single crystal. The connection of grains is enhanced by pressure to give rise to a suppression of the magnitude of the TMR.

¹H. Y. Hwang, S.-W. Cheong, N. P. Ong, and B. Batlogg, Phys. Rev. Lett. **77**, 2041 (1996).

²A. de Andrés, M. García-Hernández, and J. L. Martínez, Phys. Rev. B **60**, 7328 (1999).

³S. Lee, H. Y. Hwang, Boris I. Shraiman, W. D. Ratcliff II, and S.-W. Cheong, Phys. Rev. Lett. **82**, 4508 (1999).

⁴K. I. Kobayashi, T. Kimura, H. Sawada, K. Terakura, and Y. Tokura, Nature (London) **395**, 677 (1998).

⁵O. Chmaissem, R. Kruk, B. Dabrowski, D. E. Brown, X. Xiong, S. Kolesnik, J. D. Jorgensen, and C. W. Kimball, Phys. Rev. B **62**, 14197 (2000).

⁶K. I. Kobayashi, T. Okuda, Y. Tomioka, T. Kimura, and Y. Tokura, J. Magn. Magn. Mater. **218**, 17 (2000).

⁷Y. Tomioka, T. Okuda, Y. Okimoto, R. Kumai, K.-I. Kobayashi, and Y. Tokura, Phys. Rev. B **61**, 422 (2000).

⁸F. Honda, S. Kaji, I. Minamitake, M. Ohashi, G. Oomi, T. Eto, and T. Kagayama, J. Phys.: Condens. Matter **14**, 11501 (2002).

⁹M. García-Hernández, F. Guinea, A. de Andrés, J. L. Martínez, C. Prieto, and L. Vázquez, Phys. Rev. B **61**, 9549 (2000).

¹⁰M. Garcia-Hernandez, J. L. Martinez, M. J. Martinez-Lope, M. T. Casais, and J. A. Alonso, Phys. Rev. Lett. **86**, 2443 (2001).

¹¹H. G. Yin, J.-S. Zhou, J.-P. Zhou, R. Dass, J. T. McDevitt, and John B. Goodenough, Appl. Phys. Lett. **75**, 2812 (1999).

¹²T. Goko, Y. Endo, E. Morimoto, J. Araki, and T. Matsumoto, Physica B **329–333**, 837 (2003).